

General and feature-based semantic representations in the semantic network

Antonietta Gabriella Liuzzi ^{a*}, Aidas Aglinskas ^b, Scott Laurence Fairhall ^a

^a Center for Mind/Brain Sciences, University of Trento, Trento, 38068, Italy

^b Department of Psychology, Boston College, Boston, 02467, USA

*Corresponding author:

Antonietta Gabriella Liuzzi, PhD

Center for Mind/Brain Sciences, University of Trento, Trento,
Corso Bettini 31, I-38068-Rovereto, Italy.

E-mail: antonietta.liuzzi@unitn.it

ACKNOWLEDGEMENTS

The project was funded by the European Research Council (ERC) grant CRASK - Cortical Representation of Abstract Semantic Knowledge, awarded to Scott Fairhall under the European Union's Horizon 2020 research and innovation program (grant agreement no. 640594).

ABSTRACT

How semantic representations are manifest over the brain remains a topic of active debate. A semantic representation may be determined by specific semantic features (e.g. sensorimotor information), or may abstract away from specific features and represent generalized semantic characteristics (general semantic representation). Here we tested whether nodes of the semantic system code for a general semantic representation *and/or* possess representational spaces linked to particular semantic features. In an fMRI study, eighteen participants performed a typicality judgment task with written words drawn from sixteen different categories. Multivariate pattern analysis (MVPA) and representational similarity analysis (RSA) were adopted to investigate the sensitivity of the brain regions to semantic content and the type of semantic representation coded (general or feature-based). We replicated previous findings of sensitivity to general semantic similarity in posterior middle/inferior temporal gyrus (pMTG/ITG) and precuneus (PC) and additionally observed general semantic representations in ventromedial prefrontal cortex (PFC). Finally, two brain regions of the semantic network were sensitive to semantic features: the left pMTG/ITG was sensitive to haptic perception and the left ventral temporal cortex (VTC) to size. This finding supports the involvement of both general semantic representation and feature-based representations in the brain's semantic system.

Keywords: semantic representations, pMTG, VTC, MVPA, RSA, fMRI

1. INTRODUCTION

Conceptual and semantic knowledge are fundamental aspects of human cognition and the investigation of the neural substrates underlying these processes is an ongoing topic of research in the cognitive neurosciences. Although current evidence has demonstrated that semantic knowledge is represented in a distributed manner over the brain (Huth et al., 2016; Lambon-Ralph et al., 2017), the manner in which semantic representation is manifest remains a topic of active debate.

The association damage to the anterior temporal lobe primary progressive aphasia, herpes encephalitis and lesions led to an emphasis of this brain regions as a critical locus for semantic processing (Mummery et al, 2000, Noppeny et al, 2007). However, functional neuroimaging has suggested a broader range of regions are involved in semantic processing (Damasio et al 1996). A meta-analysis of 120 studies (Binder et al., 2009) identified a “general semantic network” - a left-lateralized network consisting of seven brain regions that were activated in a variety of semantic tasks: angular gyrus, lateral and ventral temporal cortex, ventromedial prefrontal cortex, inferior frontal gyrus, dorsal medial prefrontal cortex and the posterior cingulate gyrus. However, not all brain regions activated in semantic tasks necessarily represent semantic content, for instance regions may control access to semantic information rather than contain that information themselves (Thompson-Schill 1997; Martin and Chao 2001, Lambon-Ralph et al., 2017). Starting from this assumption, Fairhall and Caramazza (2013) identified a set of regions representing semantic content by means of Multivariate Pattern Analysis (MVPA) and Representational Similarity Analysis (RSA) (Kriegerskorte et al 2008). The authors showed that a left-lateralized network – consistent with the general semantic network - was not only recruited in a typicality judgment task, but was also able to distinguish among the conceptual representation of object categories, generalizing across input-modality (written words or pictures). In addition, among all regions composing such network, the posterior middle/inferior temporal gyrus (pMTG/ITG) and the posterior cingulate/precuneus (PC) were the only two regions showing a semantic similarity effect: similarity between neural activity pattern of pMTG/ITG and PC were representative of the semantic distance between object categories. Accordingly, Fairhall and Caramazza (2013) suggested that PC and pMTG/ITG are candidate regions for the supramodal representation of the conceptual properties of objects. However, representations in several other regions were shown to be sensitive to object category, but did not conform to a general semantic representational space. It is possible that representations in these regions are related to particular semantic features, or sets of semantic features.

Object categories are frequently characterized by specific sensory and motor information (semantic features). The embodied theories of semantics claim that the semantic processing of a concept determines the re-activation of sensory and motor information produced when the referent of a word or a sentence is actually experienced (Barsalou 2008, Meteyard and Vigliocco, 2008; Kiefer and Pulvermüller, 2012). In addition to sensory and motor information, a more recent model - the Grounded Representation in Action, Perception and Emotion Systems (GRAPES) model (Martin 2016) - suggested that the processing of a concept determines the re-activation of emotional information as well. In line with this view, it has been proposed that sensory-modality representations are located near corresponding sensory, motor and emotion networks, and by receiving bottom-up input in their modality and top-down input from other modalities, code lower-level representations. These modality-specific representations converge in higher-level cortices which bind representations from two or more modalities and code supramodal representations (Binder and Desai 2011, Fernandino et al., 2015).

Fernandino et al., (2015) investigated the role played by higher level areas by examining the activation associated with five sensorimotor features, during explicit retrieval of such sensorimotor features of written words. The results suggested a hierarchical organization of semantic memory

where bimodal, trimodal and polymodal regions bind two, three or several sensorimotor information respectively. Polymodal regions, that is regions activated by all 5 sensorimotor information (Fernandino et al., 2015), corresponded to high-level cortical hubs, such as angular gyrus, precuneus/posterior cingulate/retrosplenial cortex, parahippocampal gyrus, and medial prefrontal cortex.

Thus, on one hand it seems that semantic content may be intrinsically determined by sensorimotor information of the concept (feature-based representation) and on the other that some semantic representations are abstracted away from specific features and represent generalized semantic characteristics (general semantic representation). The current experiment aims at (1) replicating Fairhall and Caramazza (2013)'s findings and (2) probing whether different semantic features drive representation across nodes of the semantic system. We want to determine whether brain regions sensitive to semantic content, and that are able to distinguish between semantic categories, (a) code for a general semantic representation only, (b) code for a general semantic representation *and* possess representational spaces linked to particular semantic features, (c) code for particular semantic features. While the sensitivity to semantic content will be addressed by means of MVPA, the type of semantic representation (general *and/or* feature-based) will be addressed by means of RSA: By extracting information from multi-dimensional scale and by separating data into different categories, MVPA allows to determine the brain response patterns that contain semantic content. By quantifying the strength of the similarities among different neural patterns, RSA allows to identify brain regions whose brain activity is sensitive to the conceptual similarity of categories encoded (semantic representations) (Kriegeskorte et al 2008). Secondly, we will investigate whether regions outside the semantic network are sensitive to semantic features by adopting a searchlight-RSA approach.

2. MATERIALS AND METHODS

2.1 Participants

Twenty right-handed, native Italian participants (mean age $M=25.8$ $SD=4.47$, 11 females) took part in the study. Participants had normal, or corrected to normal, vision and were free from neurological disorders. All participants gave informed consent and the study was approved by the Ethics Committee of the University of Trento. Two subjects were removed from the analysis due to technical problems during fMRI acquisition.

2.2 Stimulus set

An objective, data-driven strategy was employed to generate the object categories used in this study. Original stimulus selection was corpus-based. From a large text corpus (Wikipedia), we computed the co-occurrence frequency of 1481 concrete nouns (called “targets”) with 6773 words (called “features”) consisting of common verbs, adjectives and nouns others than the 1481 targets. Word occurrences were log transformed, and the correlation distance ($1-r$) between targets was taken as a measure of word relatedness. Hierarchical cluster analysis grouped nouns into cohesive semantic categories, among which 17 were chosen. Each semantic category consisted of 24 items, which were translated to Italian. The semantic category “Leisure” containing nouns pertaining to items used for entertainment (‘radio’, ‘movie’, ‘song’, ‘journal’, etc.) was removed due to low subjective consistency between the items. The final stimulus set consisted of 16 semantic categories (Clothes, Music Instruments, Tools, Households, Materials, Transports&Movement, Animals-Water, Animals-Insects, Animals-Domestic, Animals-Wild, Animals-Birds, Fruits&Vegetables, Foods&Drinks, Flora, Outdoors and Bodyparts).

2.3 Semantic model

The semantic model was created using word embeddings generated via the word2vec word representation models trained on the Italian Wikipedia (Berardi et al, 2015). Briefly, for each stimulus an embedding vector containing 300 values was extracted and the correlation between embeddings was used to calculate item similarity. Item similarity values were then averaged across items within a category to create the category similarity model (Fig 1).

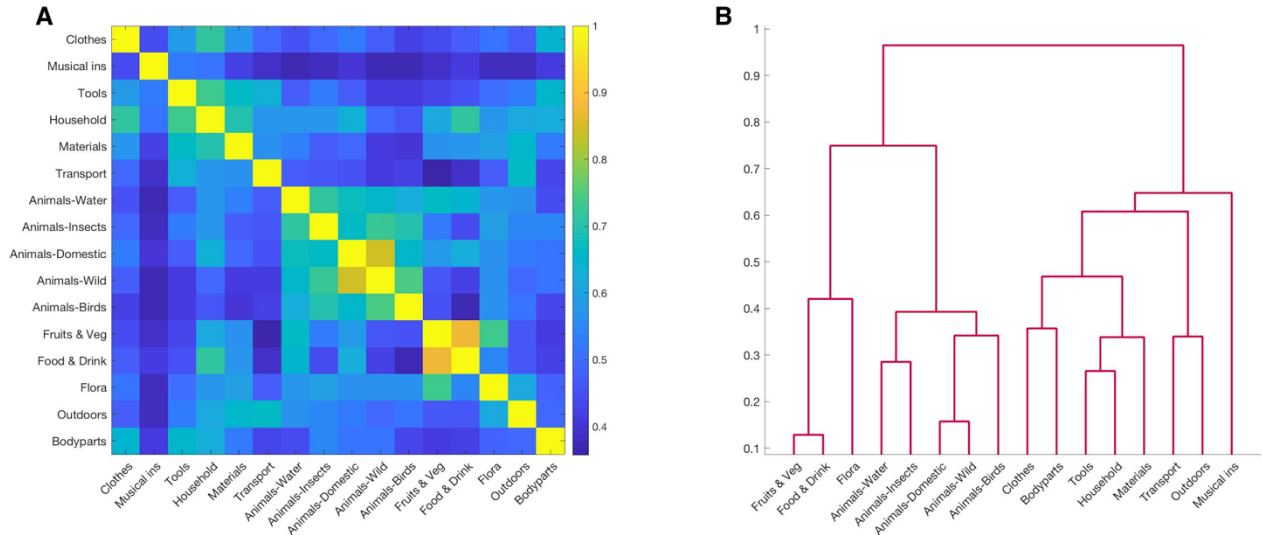


Fig 1: A. Semantic model representing the semantic similarity between 16 categories. **B.** Dendrogram of the 16 semantic categories.

2.4 Task and Experiment details

18 subjects performed a blocked fMRI experiment. Each block started with a fixation cross (duration 4s), followed by the name of the category (e.g. “Household items”) (duration 4s). Next, an additional fixation cross appeared on the screen for 2s, followed by a written word representing a concept belonging to the category (e.g. “Spatula”). During stimulus presentation (duration 2s), participants were asked to read a word and rate how typical it was for the given category (How typical is spatula of a household item). Participants rated the items on a scale from 1 (low typicality) to 4 (high typicality) using a button box.

The entire experiment consisted of 54 blocks divided in 2 sessions: 17 category blocks, one for each semantic category, and one block for a control condition which consisted of a 1-back matching task with function words. Each block was composed of eight stimulus presentations. Each block was presented three times, so that the 24 concepts belonging to the same category were presented once for each subject.

2.5 Features and feature-based models

In order to measure the extent to which semantic categories rely on the relevance of specific features, eighteen new subjects performed a behavioral task. The task started with a feature-specific question aimed at focusing the participants’ attention on the relevance of each feature for that specific concept (e.g. How easily the following items can be recognized by touch?). The question was followed by a list of 64 concepts: 4 concepts for each semantic category so that, across the 18 subjects tested, each concept was rated 3 times. Subjects were asked to place the concepts on a line from low to high values/relevance. Subjects were explicitly instructed not to order the concepts from 1 to 64, but to place the category on the arrow according to the main criteria that the distance between categories was representative of the similarity (or dissimilarity) between categories for feature’s relevance. Each subject performed the task twelve times, once for each feature. Because of 5 out of 12 feature

questions were interpreted inconsistently across participants, seven features were selected for the final feature dataset: Manipulation, haptic perception, color, taste, size, animacy and sound.

Representational dissimilarities matrices for each feature were based on the Euclidean distance between semantic categories.

2.6 Image acquisition

A SIEMENS Prisma scanner (field strength - 3 Tesla) with a 64-channel head coil provided structural and functional images. Total of 720, T2* weighted EPI scans (voxel size - 3mm, isotropic) were acquired during the experiment. The experiment was split into 2 runs, each lasting 12minutes (360 volumes). Functional scans were AC/PC aligned, and 30 axial slices (gap - 0.6mm, TR = 2000ms, TE = 28ms, image matrix = 64 64, flip angle = 75, 108mm brain coverage) were collected for each volume. For each subject, a high resolution T1 weighted MPRAGE (1mm, isotropic) anatomical scan (208 sagittal slices, flip angle 12, TR - 2140ms, TE - 2.9ms) was also acquired. Stimuli were presented on a 42", MR-compatible Nordic NeuroLab LCD monitor positioned at the back of the magnet bore that participants saw through a mirror in front of them. Stimuli were presented using a custom PsychToolBox 3 script running on top of Matlab R2017b.

3. DATA ANALYSIS

3.1 Preprocessing

Data were pre-processed with Statistical Parametric Mapping - SPM12 (Wellcome Trust Centre for Neuroimaging, University College London, UK). Functional images were realigned and resliced and a mean functional image was created. Next, the structural image was co-register with the mean function image and segmented. Functional images were normalized to the Montreal Neurological Institute (MNI) T1 space, resampled to a voxels size of 2x2x2 mm³ and spatially smoothed with 8mm FWHM kernel. Subject specific response estimates (beta weights) were derived by fitting a general linear model (GLM) to the data with 54 blocks. Estimated motion parameters from the realignment procedure were included in the model as regressors of no interest.

3.2 Whole-brain MVPA

Brain regions sensitive to semantic content were identified by means of a whole-brain MVPA. Subject-specific β weights were used as input of a whole-brain Multivoxel Pattern Analysis (MVPA). For each voxel in the brain, a spherical neighborhood of β values was defined with a variable radius including the 200 voxels nearest to the center voxel. A searchlight analysis was performed by using a linear discriminant analysis (LDA) classifier as implemented in CoSMo MVPA (<http://www.cosmomvpa.org/>) (Oosterhof et al., 2016). In order to compute classification accuracies, for each subject a classifier was trained on 32 β maps (two for each semantic category) and tested on 16 β maps (one for each semantic category) by means of a cross-validation measure with LDA classifier. A total of 3 iterations for each subject were performed: one for each repetition of the semantic categories. For each searchlight, accuracy scores from different iterations were averaged and the classification accuracy value was summarized at the center voxel of the sphere. The resulting subject-specific accuracy maps were smoothed with 6mm FWHM kernel and entered into a one-sample t test. In order to exclude voxels with relatively low signal-to-noise ratio, a group-level mask (see section "Parametric analysis") as explicit mask.

3.3 VOI definition

VOIs were extracted from the whole-brain MVPA. Only significant clusters at PFWE-CORR (cluster level) < 0.001 were selected. For each local maxima a sphere with variable radius of 20mm was created. In

order to exclude voxels where no significant decoding accuracy was detected, each VOI was intersected with the whole-brain MVPA map.

3.4 Representational Similarity Analysis

In order to determine whether regions sensitive to object category contained a representational space consistent with a general semantic representation, a classical representational similarity analysis (RSA) was applied. For each subject and for each VOI, a fMRI Representational Dissimilarity Matrix (RDM) was computed by extracting the 16 β weights patterns related to the 16 semantic categories (matrix 16xN.voxels) and computing a pair-wise correlation (similarity matrix 16x16). As each category was presented three times during the entire experiment, 3 fMRI dissimilarity matrices - one for each repetition/observation - were computed. For each subject, the 3 dissimilarity matrices were averaged and the resulting matrix was correlated with the semantic model. The significance of the results was performed by means of One-Sided t -Test.

Secondly, RSA was applied for addressing whether the same brain regions contained representational spaces linked to particular semantic features. For each feature, the fMRI RDM was correlated with a feature dissimilarity model partialling out all other features.

3.5 Searchlight RSA

We also evaluated the sensitivity of brain regions, within as well as outside the semantic network, to semantic features, by means of a searchlight RSA approach. For each subject and for each voxel of the brain, a sphere of 200 voxels was created. 16 β weights patterns related to the 16 semantic categories were extracted and a correlation between each pair of category vectors was computed, as implemented in CoSMo MVPA (<http://www.cosmomvpa.org/>) (Oosterhof et al., 2016). The obtained fMRI RDM was correlated with the model RDM. The correlation value was summarized at the center voxel of the sphere. The resulting three correlation maps, one for each repetition of the semantic category, were then averaged and smoothed with 6mm FWHM kernel. Finally, smoothed data were entered into a one-sample t test with a group-level mask (see section “Parametric analysis”) as explicit mask. Significance was set at voxel-level inference threshold of uncorrected $p < .001$ combined with cluster-level inference of $p < .05$ corrected for the whole brain volume.

3.6 Parametric analysis

In order to investigate whether sensitivity to semantic features is reflected in regional response magnitude - rather than subtle differences between voxels - a univariate analysis was performed. 12 t -contrasts were entered in a univariate second-level analysis, one for each feature: for each contrast, the regressors were weighted with normalized z -scores derived from the behavioral task (see section “Features and feature-based model”).

4. RESULTS

4.1 Behavioral results

Across 16 experimental categories, there were significant differences in reaction times, $F(15,225) = 3.952$, $p < .001$. On average, however, there were no difference between living ($n=8$) / non-living ($n=8$) category domains, $t(17) = 0.62$, $p = .545$. Typicality ratings differed across 16 categories, $F(15,225) = 15.659$, $p < .001$. Items in domestic animals’ category were rated as being less typical than other categories.

4.2 Whole-brain MVPA and VOI definition

A whole-brain MVPA revealed ten clusters sensitive to semantic category: a cluster that extended from the left intra parietal sulcus (IPS) to the posterior middle/inferior temporal lobe (pMTG/ITG) through the angular gyrus (AG); the precuneus (PC); the right AG, the left dorsolateral prefrontal cortex (PFC); the left ventral-temporal cortex (VTC); the left inferior frontal gyrus (IFG), the left and right V1; the left lateral orbital frontal cortex (OFC); the left ventromedial PFC and the left lateral PFC (Fig 2; Table 1).

Twelve local maxima were extracted from a whole-brain MVPA resulting in 12 VOIs with a cluster size that ranged between 202 and 787 voxels (Table2).

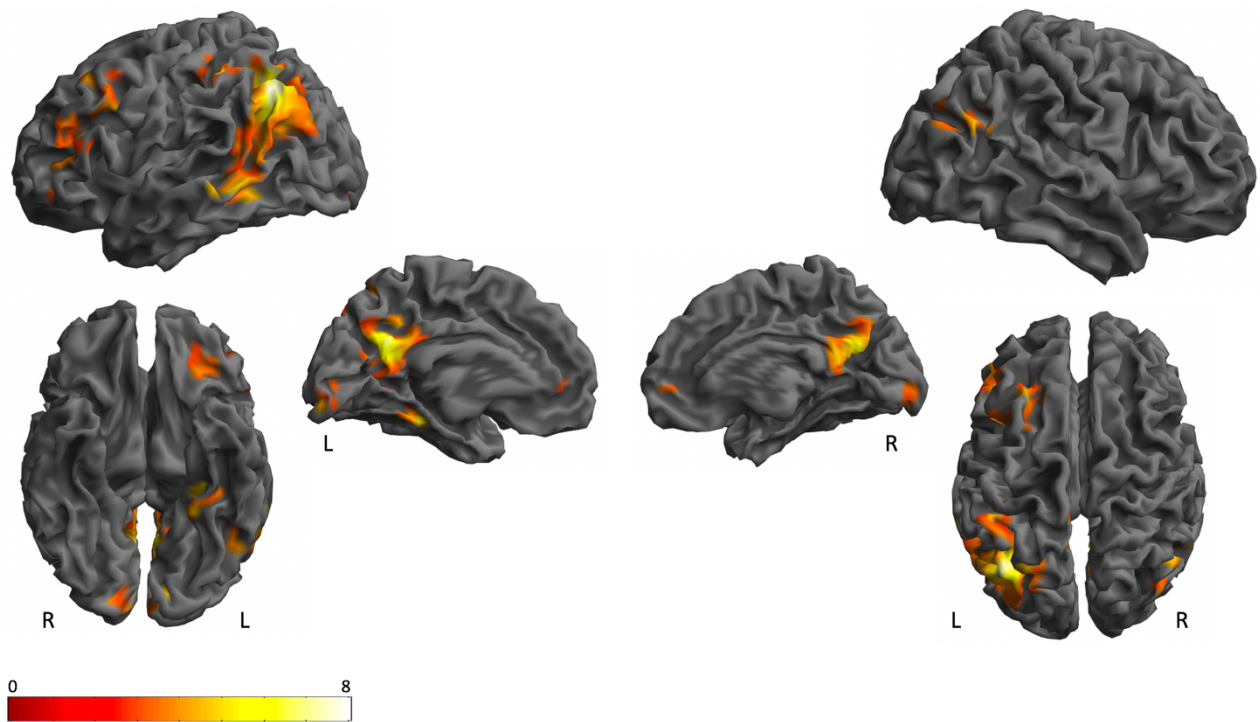


Fig 2. Whole-brain MVPA: 3D rendering, sagittal and axial slices, showing significant accuracy for a whole-brain MVPA at voxel-level inference threshold of uncorrected $p < .001$ combined with cluster-level inference of $p < .05$ corrected for the whole brain volume, extent threshold > 202 voxels. Colors represent low (red) and high (yellow) t-values.

	MNI coordinates			Extent	$P_{FWE-CORR}$ (Cluster level)
	x	y	z		
L posterior parietal-temporal cortex	-26	-64	46	3829	0.000
PC	-4	-56	28	2341	0.000
R AG	58	-60	24	291	0.009
L VTC	-32	-32	-16	309	0.007
L IFG	-50	40	6	519	0.000
L dorsolateral PFC	-28	24	36	367	0.003

L and R V1	18	-90	-4	462	0.001
L lateral PFC	-44	12	32	221	0.027
L ventromedial PFC	-8	44	2	202	0.038
L lateral OFC	-28	28	-12	234	0.022

Table 1: MVPA: Cluster showing significant accuracy for a whole-brain MVPA at voxel-level inference threshold of uncorrected $p < .001$ combined with cluster-level inference of $p < .05$ corrected for the whole brain volume. Extent refers to the number of $2 \times 2 \times 2 \text{ mm}^3$ voxels. *Abbreviations:* L: left; R: right; PC: Precuneus; AG: angular gyrus; VTC: ventral temporal cortex; IFG: inferior frontal gyrus; PFC: pre-frontal cortex; OFC: orbitofrontal cortex.

VOI	Local Maxima			Size $2 \times 2 \times 2 \text{ mm}^3$
	x	y	z	
L pMTG/ITG	-58	-52	-10	555
L AG	-52	-64	28	787
L IPS	-26	-64	46	669
PC	-4	-56	28	707
R AG	58	-60	24	202
L VTC	-32	-32	-16	307
L IFG	-50	40	6	501
L dorsolateral PFC	-28	24	36	374
L and R V1	18	-90	-4	294
L lateral PFC	-44	12	32	225
L ventromedial PFC	-8	44	2	202
L lateral OFC	-28	28	-12	234

Table 2: VOIs extracted from the whole-brain MVPA. Size refers to a $2 \times 2 \times 2 \text{ mm}^3$ voxels. *Abbreviations:* L: left; R: right; PC: Precuneus; AG: angular gyrus; VTC: ventral temporal cortex; IFG: inferior frontal gyrus; PFC: pre-frontal cortex; OFC: orbitofrontal cortex.

4.3 Representational Similarity Analysis – Neural and General Semantic Similarity

A priori pMTG/ITG and PC revealed significant semantic similarity effects in both regions (pMTG/ITG: $r = 0.07$; $p = .002$; PC: $r = 0.07$; $p = .008$). Moreover, the effect remained significant after regressing out all sensory-motor features (pMTG/ITG: $p = .03$; PC: $p = .007$). Significant effects were also seen in ventromedial PFC ($r = 0.09$, $p = .002$), which survived Bonferroni correction for number of regions. Weaker effects that would not survive correction were present in lateral OFC ($r = 0.07$, $p = .007$), right AG ($r = 0.07$; $p = .01$), left AG ($r = 0.05$; $p = .02$) and left VTC ($r = 0.05$; $p = .03$) (Table 3).

	r	$p\text{-value}$
L pMTG/ITG	0.07	.002
L ventromedial PFC	0.09	.002
L lateral OFC	0.07	.007
PC	0.07	.008
R AG	0.07	.01
L AG	0.05	.02
L VTC	0.05	.03
L IFG	0.03	.16
L dorsolateral PFC	0.02	.17
L and R V1	0.01	.29
L lateral PFC	0.003	.46
L IPS	-0.01	.68

Table 3: Semantic similarity effects based on RSA. Values surviving a Bonferroni correction for number of regions at $p < .05$ are reported in bold. *Abbreviations:* L: left; R: right; pMTG/pITG: posterior middle and inferior temporal gyrus; PFC: pre-frontal cortex; OFC: orbitofrontal cortex; PC: precuneus; AG: angular gyrus; VTC: ventral temporal cortex; IFG: inferior frontal gyrus; IPS: inferior parietal sulcus.

4.4 Representational Similarity Analysis – Neural and Feature-based Similarity

Sensitivity of the selected brain regions for features was investigated by means of RSA. For each feature tested, all remaining features were partialled out. While the left VTC was sensitive to size ($r = 0.14, p = .00003$), the pMTG/ITG was sensitive to haptic perception ($r = 0.13, p = .0004$) (Fig 3). These effects remained significant after a Bonferroni correction for number of features. At more lenient uncorrected thresholds, significant effects were present for haptic perception at $p < 0.05$ in left VTC ($r = 0.1, p = .008$) and left IPS ($r = 0.07, p = .01$). Left IFG and left ventromedial PFC were both sensitive to sound ($r = 0.07, p = .03$; $r = 0.1, p = .02$, respectively) and color ($r = 0.05, p = .05$; $r = 0.07, p = .02$, respectively), while left pMTG/ITG ($r = 0.05, p = .03$) and the dorsolateral PFC were sensitive only to color ($r = 0.06, p = .03$). Finally, the left OFC was sensitive to taste ($r = 0.1, p = .03$) and sound ($r = 0.07, p = .04$).

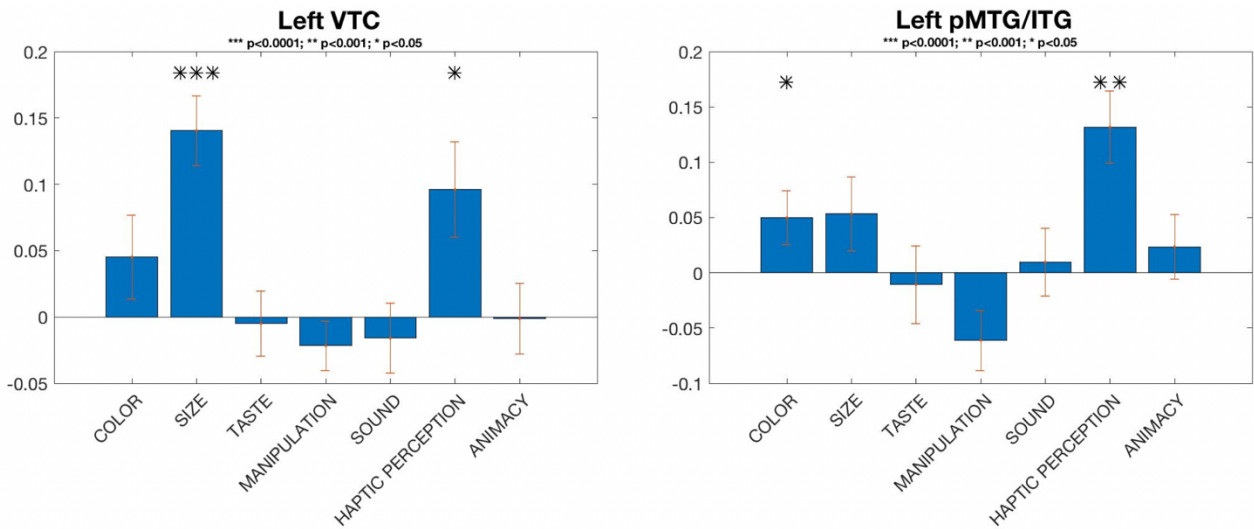


Fig 3: Features-based RSA: each bar shows an average correlation across subjects between fMRI-RDM and feature-RDM partialling out all other features. Error bar: Standard Error of the Mean (SEM).

When the semantic similarity effect in left pMTG/ITG was recomputed by partialling out the sensitivity to haptic perception, the effect was still significant ($p = .05$). Unlike the pMTG/ITG, the semantic similarity effect in left VTC no longer reached significance ($p = .2$) after partialling out the sensitivity to size.

4.5 Searchlight RSA

To confirm the ROI analysis and determine if additional brain regions represent semantic features, we performed a whole brain RSA analysis for each feature. Among all features tested, searchlight RSA revealed 2 significant clusters that are sensitive to haptic perception and size: the left pMTG/ITG (local maxima: $x = -34, y = -40, z = -20$; $KE = 945$; $PFWE-CORR = 0.001$) and left VTC (local maxima: $x = -30, y = -40, z = -20$; $KE = 565$; $PFWE-CORR = 0.004$), respectively (Fig 4).

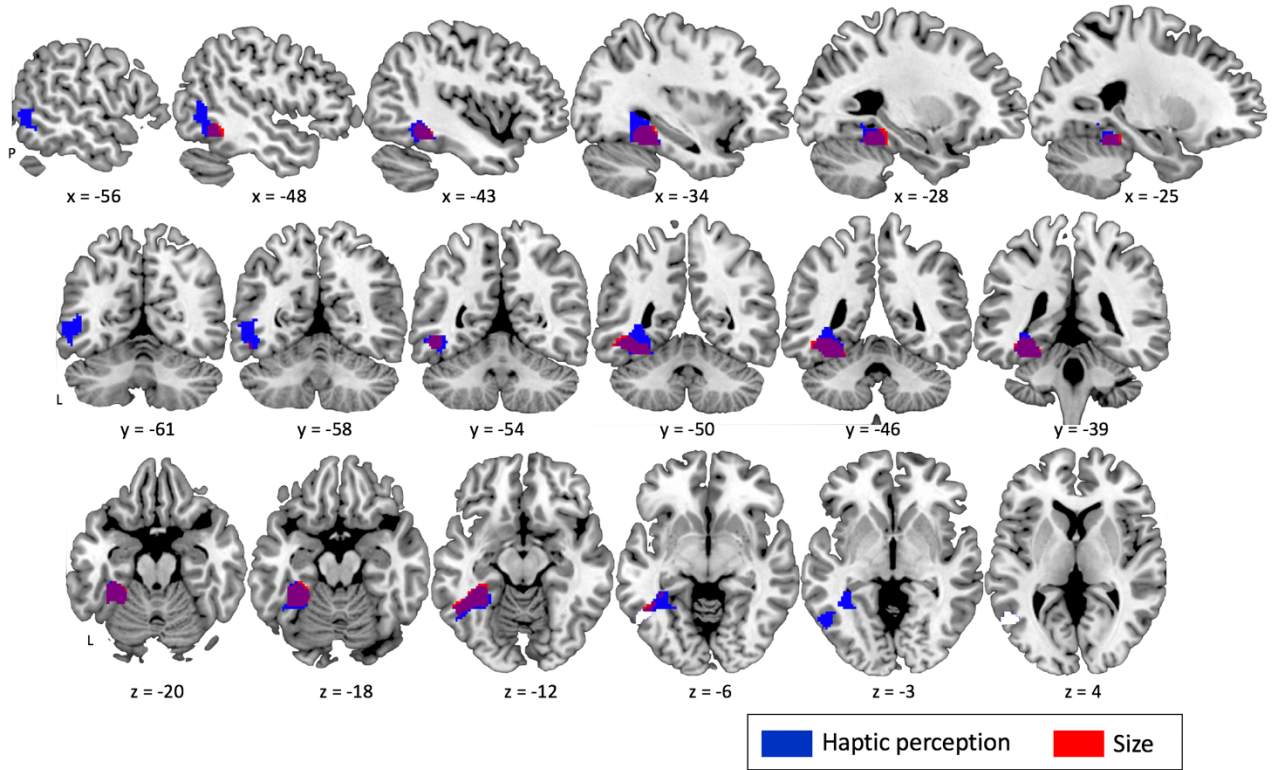


Fig 4: Searchlight RSA: Binary clusters sensitive to haptic perception (blue) and size (red).

4.6 Parametric analysis

As feature-based representation was only weakly represented in the subtle voxel-wise pattern of the response, we tested whether regions weighted towards particular features were better captured in terms of the overall amplitude of their response, rather than subtle differences between voxels. A parametric analysis was conducted for each feature, whereby the univariate regressors were weighted with scores for each feature. Only the feature size, significantly predicted the amplitude of the voxel response, in left ($x = -26$, $y = -38$, $z = -14$; $KE = 621$; $PFWE-CORR = 0.001$) and right VTC ($x = 32$, $y = -34$, $z = -16$; $KE = 482$; $PFWE-CORR = 0.005$) and in the retrosplenial cortex ($x = -10$, $y = -56$, $z = 14$; $KE = 1379$; $PFWE-CORR = 0.000$) (Fig 5). The other features did not yield any significant cluster.

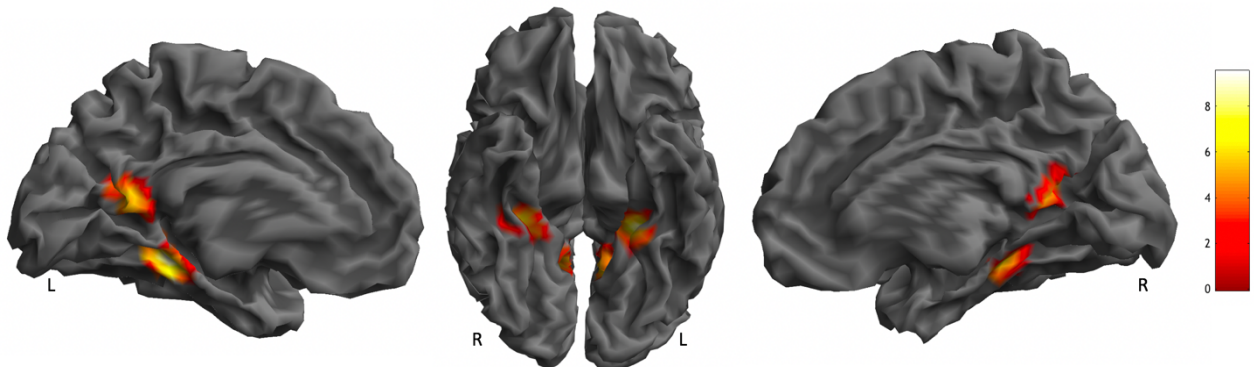


Fig 5: Parametric analysis: 3D rendering, sagittal and axial slices, showing significant clusters positively correlated with scores for size.

5. DISCUSSION

In this study, we sought to determine which regions sensitive to object category contain a representational space consistent with a general semantic representation *and/or* possess representational spaces linked to particular semantic features. MVPA identified a distributed network of generally left lateralized brain regions able to distinguish among object categories consistent with the general semantic network (Binder et al., 2009) (Fig. 2; Table 1). RSA revealed that general semantic similarity predicted neural similarity reliably in left pMTG/ITG and PC, replicating Fairhall and Caramazza (2013), as well as in the ventromedial PFC and left OFC (Table 3). When we investigated whether different features affected the semantic representations in regions composing the semantic network, the left pMTG/ITG was sensitive to haptic perception and the left VTC to size (Fig. 3).

Convergent evidence supports the role of the pMTG/ITG as a core semantic region (Binder et al., 2009): neuroimaging studies found significant activation in pMTG in response to tasks probing semantic processing in several input modalities (written words and pictures (Vandenberghe et al., 1996), auditory words (Hickok and Poeppel, 2004) and tactile inputs (Stoeckel et al., 2003)). By means of repetitive transcranial magnetic stimulation (rTMS), Hoffman et al. (2012) showed an involvement of the pMTG in both verbal and non-verbal semantic processing. Finally, lesion studies emphasized the relevance of this brain region in language comprehension at word level (Dronkers et al., 2004, Turken and Dronkers 2011). However, this central role of pMTG/ITG in semantic processing does not necessitate an involvement in coding semantic representations. It might reflect retrieval/selection operations performed on semantic content (Whitney et al., 2011) or semantic control processes under the control semantic cognition (CSC) model (Lambon-Ralph et al., 2017). Under this model, the pMTG, along with the left PFC, IPS, pre-SMA and ventromedial PFC, is involved in semantic control demands. This is in apparent contrast to the current finding where the conformation of neural representational spaces with semantic representational spaces strongly supports the encoding of semantic content within this region. However, many brain regions are characterized by heterogeneity of function leading to the non-mutually exclusive possibility that the pMTG have a role in both representation and control.

Similarly to pMTG/ITG, RSA results revealed a semantic similarity effect in PC. Evidence supports a role of the PC in semantic processing (Binder et al., 2009), internalized “default mode” (Fox et al., 2005), episodic memory (Gobbini and Haxby, 2007; Binder et al., 2009) and semantic control (Corbett et al., 2012). While the involvement of the PC in coding conceptual representation is uncertain, the strong relationship between neural and conceptual representational spaces evident in the current work, Fairhall and Caramazza (2013) as well as Liuzzi et al., (2017), provides compelling evidence that the PC plays also a role in conceptual representation.

Besides pMTG/ITG and PC, a semantic similarity effect was found in the frontal cortex, namely in the ventromedial PFC and left lateral OFC. Both ventromedial PFC and lateral OFC are strongly connected to the medial temporal cortex and activated in many semantic contrasts (Binder et al., 2009, Zald et al., 2012). With regards to the ventromedial PFC, recent evidence highlighted its contribution to reward-guided learning and decision-making (Rushworth et al., 2011), semantic control demands (Lambon-Ralph et al., 2017) and memory consolidation (Nieuwenhuis et al., 2011). More in detail, Nieuwenhuis et al., (2011) proposed that the ventromedial PFC is an integrative region receiving information about value of items from perirhinal cortex and lateral orbitofrontal cortex and contextual information from parahippocampal cortex and medial prefrontal cortex. In this sense, it is a region able to represent the value of items and their associated actions based on what is known about the current context. Similarly to the ventromedial PFC, the lateral OFC plays a crucial role in emotion, decision-making (Bechara et al. 2000) as well as in semantic monitoring/discrimination tasks (Zald et al., 2012). Although further research is needed, current results show that both ventromedial PFC and lateral OFC are strongly involved in coding general semantic representations.

Additionally, weaker semantic similarity effects were seen at lenient uncorrected threshold ($p < .05$) in left AG and a homologous region in the right hemisphere as well as the VTC. While caution must be taken in interpreting these effects, this seems to suggest that general semantic representation may be more widespread than previously thought (Fairhall and Caramazza, 2013). The AG had been implicated in integrating conceptual information (Binder et al., 2009, Bonner et al., 2013) as well as combinatorial processing (Price et al., 2015). While the posterior section of the VTC observed here is frequently implicated in semantic processing (Binder et al., 2009), no activation was detected in the anterior section of the VTC, which may result from low signal to noise in this region in the scan sequence we used (Devlin et al., 2000).

The second goal of the current experiment was the investigation of whether different semantic features drive the representation across nodes of the semantic system. Two brain regions of the semantic network were sensitive to semantic features: after partialling out all other features, the left pMTG/ITG was sensitive to haptic perception and the left VTC to size (Fig. 4).

In addition to being implicated in semantic representation (Fairhall and Caramazza 2013) and control (Lambon-Ralph et al., 2017), the pMTG is also involved in hand and non-hand actions observation and imitation (Caspers et al., 2010), action perception and understanding (Urgesi et al., 2014) visual action and action knowledge (Wurm and Caramazza 2018) and tool recognition (Ishibashi et al., 2016) and lesions to pMTG are associated with tool related semantic deficits (Damasio, 1996). While our current results show a sensitivity to haptic perception, a previous study on sensorimotor features (Fernandino et al., 2015), showed that the left pMTG was sensitive to sound and visual motion. Such discrepancy in sensitivity of this brain region to specific semantic features might be explained in terms of task: while Fernandino et al. (2015) used an explicit retrieval of sensorimotor information, we adopted a typicality judgment task which encourages most prototypical semantic access for that feature.

In order to test whether the general semantic similarity effect in the left pMTG/ITG was influenced by the sensitivity of this brain region to a specific features (e.g. haptic perception), the correlation between the semantic model and the fMRI data (RSA) was recomputed by first partialling out the effect for all features and secondly by partialling out the effect for haptic perception: As the semantic similarity effect was still significant, our results prove the involvement of the left pMTG/ITG in coding general semantic relationships beyond feature representation (Fairhall and Caramazza 2013). While the pMTG/ITG was sensitive to haptic information, the left VTC was sensitive to size. Although lateral and ventral temporal cortex are considered heteromodal regions involved in concept retrieval and supramodal integration (Binder et al., 2009), a more recent theory - the Posterior Medial Anterior Temporal (PMAT) model (Ranganath & Ritchey, 2012; Ritchey et al., 2015) – proposed an anatomical and functional distinction between the anterior and the posterior portion of the medial temporal cortex, each belonging to distinct cortico-hippocampal networks. According to the PMAT model, perirhinal cortex and parahippocampal cortex are core components of the anterior and the posterior portion of the medial temporal cortex, respectively. At functional level, while the anterior portion is involved in item-based memory, the posterior portion is instead implicated in spatial navigation, episodic retrieval and situational models. However, the posterior VTC is also characterized by large-object selectivity: while left PHC is sensitive to scenes (Epstein 2008), to access to place-related semantic knowledge (Fairhall and Caramazza 2013b, Fairhall, et al., 2014, Aglinskis and Fairhall, 2019), to salient objects that are part of specific scene (Maguire et al., 1998, 2001), it is also sensitive to big, compared to small, objects (Konkle and Oliva, 2012). Interestingly, studies on blind population (He et al., 2013, Wang et al., 2015) showed that such large-object selectivity of the PHC does not require visual processing or even visual experience: compared to tools and animals, large nonmanipulable objects activated the PHC in both sighted and blind people (He et al., 2013). The current finding that representational spaces in this region conforms to size relationships between object-categories indicates the importance of feature-based semantic representation in this region.

While general semantic representation of multiple categories and features may be represented on a fine neural scale, allowing the simultaneous representations of multiple semantic dimensions, regions specialized for a particular feature like size may be more homogenous and their input into the representation represented in their overall response. We tested this hypothesis by means of a parametric analysis where – for each feature – the univariate regressors were weighted with normalized z-feature-scores. Besides the PHC, this parametric analysis revealed a sensitivity to size in the RSC as well. Similarly to PHC, RSC is involved in spatial navigation, scene (Maguire 2001b, Epstein et al., 2008) as well as physical size (Park et al., 2014). By investigating two scene properties, namely physical size and functional clutter (the organization and quantity of objects that fill up the space), Park et al., (2014) demonstrated that while parahippocampal place area (PPA) was sensitive to both size and clutter, RSC showed much stronger pattern sensitivity to size only. Our parametric results were slightly more robust (PHC: peak-level $T = 9.52$) than a pattern-based analysis (PHC: peak-level $T = 9.31$), supporting the idea that parametric models seem to capture feature-based effects more than pattern-based analyses. Thus, general semantic representation may be represented in the fine scale pattern of activation within a region, while uni-dimensional features represented in a specialized region may contribute to representation through their overall level of activity.

6. CONCLUSIONS

The current finding supports a model of generalized and specialized semantic representation. Firstly and importantly, we replicate previous findings of general representation of objects that conform to their overall semantic similarity in the left pMTG/ITG and PC (Fairhall & Caramazza, 2013) and extend these findings to show additional representations in vmPFC. Furthermore, we report that this system is complemented by representations that are weighted towards particular features: the left pMTG/ITG is sensitive to haptic perception and the left VTC to size. The nature of feature-based and generalized semantic representation may differ in that the feature is encoded within the whole region rather than subtle variation in the pattern of the response across voxels.

Bibliography

1. Aglinskas, A., & Fairhall, S. L. (2019). Regional Specialization and Coordination Within the Network for Perceiving and Knowing About Others. *Cerebral Cortex*.
2. Barsalou LW. 2008. Grounded cognition. *Annu Rev Psychol*. 59:617–645
3. Bechara, A., Damasio, H., & Damasio, A. R. (2000). Emotion, decision making and the orbitofrontal cortex. *Cerebral cortex*, 10(3), 295-307.
4. Berardi, G., Esuli, A., & Marcheggiani, D. (2015, May). Word Embeddings Go to Italy: A Comparison of Models and Training Datasets. In *IIR*.
5. Binder, J. R., & Desai, R. H. (2011). The neurobiology of semantic memory. *Trends in cognitive sciences*, 15(11), 527-536.
6. Binder, J. R., Desai, R. H., Graves, W. W., & Conant, L. L. (2009). Where is the semantic system? A critical review and meta-analysis of 120 functional neuroimaging studies. *Cerebral Cortex*, 19(12), 2767-2796.
7. Bonner, M. F., Peelle, J. E., Cook, P. A., & Grossman, M. (2013). Heteromodal conceptual processing in the angular gyrus. *Neuroimage*, 71, 175-186.
8. Caspers, S., Zilles, K., Laird, A. R., & Eickhoff, S. B. (2010). ALE meta-analysis of action observation and imitation in the human brain. *Neuroimage*, 50(3), 1148-1167.
9. Corbett, F., Jefferies, E., Burns, A., & Lambon-Ralph, M. A. (2012). Unpicking the semantic impairment in Alzheimer's disease: qualitative changes with disease severity. *Behavioural neurology*, 25(1), 23-34.
10. Damasio, H., Grabowski, T. J., Tranel, D., Hichwa, R. D., & Damasio, A. R. (1996). A neural basis for lexical retrieval. *Nature*, 380(6574), 499-505.
11. Devlin, J. T., Russell, R. P., Davis, M. H., Price, C. J., Wilson, J., Moss, H. E., Matthews P.M. & Tyler, L. K. (2000). Susceptibility-induced loss of signal: comparing PET and fMRI on a semantic task. *Neuroimage*, 11(6), 589-600.
12. Dronkers, N. F., Wilkins, D. P., Van Valin, R. D. Jr., Redfern, B. B., and Jaeger, J. J. (2004). Lesion analysis of the brain areas involved in language comprehension. *Cognition* 92, 145–177.
13. Epstein, R. A. (2008). Parahippocampal and retrosplenial contributions to human spatial navigation. *Trends in cognitive sciences*, 12(10), 388-396.
14. Fairhall, S. L., Anzellotti, S., Ubaldi, S., & Caramazza, A. (2014). Person-and place-selective neural substrates for entity-specific semantic access. *Cerebral Cortex*, 24(7), 1687-1696.
15. Fairhall, S. L., & Caramazza, A. (2013). Brain regions that represent amodal conceptual knowledge. *Journal of Neuroscience*, 33(25), 10552-10558.
16. Fairhall, S. L., & Caramazza, A. (2013b). Category-selective neural substrates for person-and place-related concepts. *Cortex*, 49(10), 2748-2757.
17. Fernandino, L., Binder, J. R., Desai, R. H., Pendl, S. L., Humphries, C. J., Gross, W. L., ... & Seidenberg, M. S. (2015). Concept representation reflects multimodal abstraction: A framework for embodied semantics. *Cerebral Cortex*, 26(5), 2018-2034.
18. Fox, M. D., Snyder, A. Z., Vincent, J. L., Corbetta, M., Van Essen, D. C., & Raichle, M. E. (2005). The human brain is intrinsically organized into dynamic, anticorrelated functional networks. *Proceedings of the National Academy of Sciences*, 102(27), 9673-9678.
19. Gobbini, M. I., & Haxby, J. V. (2007). Neural systems for recognition of familiar faces. *Neuropsychologia*, 45(1), 32-41.
20. He, C., Peelen, M. V., Han, Z., Lin, N., Caramazza, A., & Bi, Y. (2013). Selectivity for large nonmanipulable objects in scene-selective visual cortex does not require visual experience. *Neuroimage*, 79, 1-9.
21. Hickok, G., & Poeppel, D. (2004). Dorsal and ventral streams: a framework for understanding aspects of the functional anatomy of language. *Cognition*, 92(1-2), 67-99.
22. Hoffman, P., Pobric, G., Drakesmith, M., & Lambon-Ralph, M. A. (2012). Posterior middle temporal gyrus is involved in verbal and non-verbal semantic cognition: Evidence from rTMS. *Aphasiology*, 26(9), 1119-1130.
23. Huth, A. G., De Heer, W. A., Griffiths, T. L., Theunissen, F. E., & Gallant, J. L. (2016). Natural speech reveals the semantic maps that tile human cerebral cortex. *Nature*, 532(7600), 453.
24. Ishibashi, R., Pobric, G., Saito, S., & Lambon-Ralph, M. A. (2016). The neural network for tool-related cognition: an activation likelihood estimation meta-analysis of 70 neuroimaging contrasts. *Cognitive Neuropsychology*, 33(3-4), 241-256.
25. Kiefer, M., & Pulvermüller, F. (2012). Conceptual representations in mind and brain: theoretical developments, current evidence and future directions. *cortex*, 48(7), 805-825.
26. Konkle, T., & Oliva, A. (2012). A real-world size organization of object responses in occipitotemporal cortex. *Neuron*, 74(6), 1114-1124

27. Kriegeskorte, N., Mur, M., & Bandettini, P. A. (2008). Representational similarity analysis-connecting the branches of systems neuroscience. *Frontiers in systems neuroscience*, 2, 4.
28. Lambon-Ralph, M. A., Jefferies, E., Patterson, K., & Rogers, T. T. (2017). The neural and computational bases of semantic cognition. *Nature Reviews Neuroscience*, 18(1), 42.
29. Liuzzi, A. G., Bruffaerts, R., Peeters, R., Adamczuk, K., Keuleers, E., De Deyne, S., ... & Vandenberghe, R. (2017). Cross-modal representation of spoken and written word meaning in left pars triangularis. *NeuroImage*, 150, 292-307.
30. Maguire, E. (2001). The retrosplenial contribution to human navigation: a review of lesion and neuroimaging findings. *Scandinavian journal of psychology*, 42(3), 225-238.
31. Maguire, E. A., Frith, C. D., Burgess, N., Donnett, J. G., & O'keefe, J. (1998). Knowing where things are: Parahippocampal involvement in encoding object locations in virtual large-scale space. *Journal of cognitive neuroscience*, 10(1), 61-76
32. Maguire, E. A., Frith, C. D., & Cipolotti, L. (2001). Distinct neural systems for the encoding and recognition of topography and faces. *Neuroimage*, 13(4), 743-750.
33. Martin, A. (2016). GRAPES—Grounding representations in action, perception, and emotion systems: How object properties and categories are represented in the human brain. *Psychonomic bulletin & review*, 23(4), 979-990.
34. Martin, A., & Chao, L. L. (2001). Semantic memory and the brain: structure and processes. *Current opinion in neurobiology*, 11(2), 194-201.
35. Meteyard, L., & Vigliocco, G. (2008). The role of sensory and motor information in semantic representation: A review. In *Handbook of Cognitive Science* (pp. 291-312). Elsevier.
36. Mummary, C. J., Patterson, K., Price, C. J., Ashburner, J., Frackowiak, R. S., & Hodges, J. R. (2000). A voxel-based morphometry study of semantic dementia: relationship between temporal lobe atrophy and semantic memory. *Annals of neurology*, 47(1), 36-45.
37. Nieuwenhuis, I. L., & Takashima, A. (2011). The role of the ventromedial prefrontal cortex in memory consolidation. *Behavioural brain research*, 218(2), 325-334.
38. Noppeney, U., Patterson, K., Tyler, L. K., Moss, H., Stamatakis, E. A., Bright, P., ... & Price, C. J. (2007). Temporal lobe lesions and semantic impairment: a comparison of herpes simplex virus encephalitis and semantic dementia. *Brain*, 130(4), 1138-1147.
39. Oosterhof, N. N., Connolly, A. C., & Haxby, J. V. (2016). CoSMoMvPA: multi-modal multivariate pattern analysis of neuroimaging data in Matlab/GNU Octave. *Frontiers in neuroinformatics*, 10, 27.
40. Park, S., Konkle, T., & Oliva, A. (2014). Parametric coding of the size and clutter of natural scenes in the human brain. *Cerebral cortex*, 25(7), 1792-1805.
41. Price, A. R., Bonner, M. F., Peelle, J. E., & Grossman, M. (2015). Converging evidence for the neuroanatomic basis of combinatorial semantics in the angular gyrus. *Journal of Neuroscience*, 35(7), 3276-3284.
42. Ranganath, C., & Ritchey, M. (2012). Two cortical systems for memory-guided behaviour. *Nature Reviews Neuroscience*, 13(10), 713.
43. Ritchey, M., Montchal, M. E., Yonelinas, A. P., & Ranganath, C. (2015). Delay-dependent contributions of medial temporal lobe regions to episodic memory retrieval. *Elife*, 4, e05025
44. Rushworth, M. F., Noonan, M. P., Boorman, E. D., Walton, M. E., & Behrens, T. E. (2011). Frontal cortex and reward-guided learning and decision-making. *Neuron*, 70(6), 1054-1069.
45. Stoeckel, M. C., Weder, B., Binkofski, F., Buccino, G., Shah, N. J., & Seitz, R. J. (2003). A fronto-parietal circuit for tactile object discrimination: an event-related fMRI study. *Neuroimage*, 19(3), 1103-1114.
46. Thompson-Schill, S. L., D'Esposito, M., Aguirre, G. K., & Farah, M. J. (1997). Role of left inferior prefrontal cortex in retrieval of semantic knowledge: a reevaluation. *Proceedings of the National Academy of Sciences*, 94(26), 14792-14797.
47. Turken, U., & Dronkers, N. F. (2011). The neural architecture of the language comprehension network: converging evidence from lesion and connectivity analyses. *Frontiers in systems neuroscience*, 5.
48. Urgesi, C., Candidi, M., & Avenanti, A. (2014). Neuroanatomical substrates of action perception and understanding: an anatomic likelihood estimation meta-analysis of lesion-symptom mapping studies in brain injured patients. *Frontiers in human neuroscience*, 8, 344.
49. Vandenberghe, R., Price, C., Wise, R., Josephs, O., & Frackowiak, R. S. J. (1996). Functional anatomy of a common semantic system for words and pictures. *Nature*, 383(6597), 254.
50. Wang, X., Peelen, M. V., Han, Z., He, C., Caramazza, A., & Bi, Y. (2015). How visual is the visual cortex? Comparing connectional and functional fingerprints between congenitally blind and sighted individuals. *Journal of Neuroscience*, 35(36), 12545-12559.

51. Whitney, C., Kirk, M., O'Sullivan, J., Lambon-Ralph, M. A., & Jefferies, E. (2010). The neural organization of semantic control: TMS evidence for a distributed network in left inferior frontal and posterior middle temporal gyrus. *Cerebral Cortex*, 21(5), 1066-1075.
52. Wurm, M., & Caramazza, A. (2018). Representation of action concepts in left posterior temporal cortex that generalize across vision and language.
53. Zald, D. H., McHugo, M., Ray, K. L., Glahn, D. C., Eickhoff, S. B., & Laird, A. R. (2012). Meta-analytic connectivity modeling reveals differential functional connectivity of the medial and lateral orbitofrontal cortex. *Cerebral cortex*, 24(1), 232-248.